Extended abstract, 17th Conference on Numerical Weather Prediction
August 1-5, 2005, Washington DC.

13A. 4

Analysis and Impact of Super-obbed Doppler Radial Velocity in the NCEP Grid-point Statistical Interpolation (GSI) Analysis System

Shun Liu[1], Ming Xue[1,2], Jidong Gao[1,2] and David Parrish[3]
[1]Center for Analysis and Prediction of Storms and [2]School of Meteorology
University of Oklahoma, Norman OK 73019
[3]Environmental Modeling Center, National Centers for Environmental Prediction
Camp Spring, MD 20746-4304

1. Introduction

Weather Doppler radar has the capability to scan large volumes of the atmosphere at high spatial and temporal resolutions. The real time access to the data from the entire WSR-88D network made possible by the fast internet now provides an unprecedented opportunity for using the data in operational numerical weather prediction (NWP) models. However, because of the huge volumes of radar data, the current operational data assimilation system cannot directly assimilate all of them. The relatively low resolutions of the current operational models also make the assimilation of full-volume data unnecessary. The fact that the definition of the radial velocity changes with the position of data relative to the radar poses an additional challenge not present with most other types of data; special treatment is therefore needed.

The super-obbing technique is developed by Purser et al. (2000) to reduce redundant information in the observational data as well as the data density. In this paper, a "super-obbing" technique is used to preprocess the Level-II WSR-88D radar data (Parrish 2005) for thinning and combining radar radial velocity data. The "super-obbed" data are then analyzed in the NCEP unified GSI (Grid-point Statistical Interpolation) analysis system. The impact of the super-obbed data on the analysis is examined in this paper.

2. Radar data "super-obbing" and GSI

a. Radar radial velocity "super-obbing"

In the current version of GSI, vertical velocity is not analyzed, so the more general form of superob presented here is approximated by assuming vertical velocity is zero. It is planned to eventually include vertical velocity in GSI.

Parrish (2005) applies this technique to produce radar radial velocity "super observations" (superobs, hereafter). In Parrish (2005), the radar radial velocity is given by

$$v_r(\mathbf{x}) = ud^x + vd^y + wd^z \tag{1}$$

where $\mathbf{x} = (x, y, z)$, $(d^x, d^y, d^z) = [(x - x_r)/r_d, (y - y_r)/r_d, (z - z_r)/r_d]$ are direction cosines , $r_d = [(x - x_r)^2, (y - y_r)^2, (z - z_r)^2]^{1/2}$ is the radial distance from radar, and (x_r, y_r, z_r) defines the radar position in the analysis domain. The velocity in a given domain can be represented by vector $\mathbf{a} = (u, v, w)^T$ at superob centroid of the domain. The projection of the radial velocity field in the observation space is a vector defined by

$$\mathbf{y} = [v_r(\mathbf{x}_m) \mid m = 1, 2, ...M], \tag{2}$$

where M is the total number of the radial velocity observations in the given domain. Substituting (1) to (2) gives

$$\mathbf{y} = H\mathbf{a}, \tag{3}$$

where

$$H \equiv \begin{bmatrix} d^x(\mathbf{x}_1) & d^y(\mathbf{x}_1) & d^z(\mathbf{x}_1) \\ \cdots & \cdots & \cdots \\ d^x(\mathbf{x}_M) & d^y(\mathbf{x}_M) & d^z(\mathbf{x}_M) \end{bmatrix}.$$

To reduce the dimension of the observation in the given domain, a Gram-Schmidt algorithm is applied to decompose H,

$$H = G\hat{H}, \tag{4}$$

where G and $\hat{H}$ are $M \times 3$ and 3×3 matrices, respectively. G is defined so that

$$\hat{R}^{-1} = G^T R^{-1} G\,, \tag{5}$$

* *Corresponding author address*: Shun Liu, CAPS, University of Oklahoma, Norman, OK, 73019
Shun.Liu@ou.edu

where R is the observation error covariance matrix and $\hat{R}$ is superobs error covariance matrix. The superobs in this given domain can be expressed by

$$\hat{\mathbf{y}} = \hat{R}G^T R^{-1}\mathbf{y} \,. \tag{6}$$

The forward model for superobs is given

$$\hat{\mathbf{y}} = \hat{H}a \,. \tag{7}$$

Thus, the superob reduces M pieces of information to 3.. The detailed description of forming superobs can be found in Purser et al. (2000) and Parrish (2005). Clearly, the size of the given domain for super-obbing (called super-ob grid resolution hereafter) decides the dimension of the observation space M. The super-ob grid resolution will impact the quality of the superobs, which will be investigated using the numerical experiments.

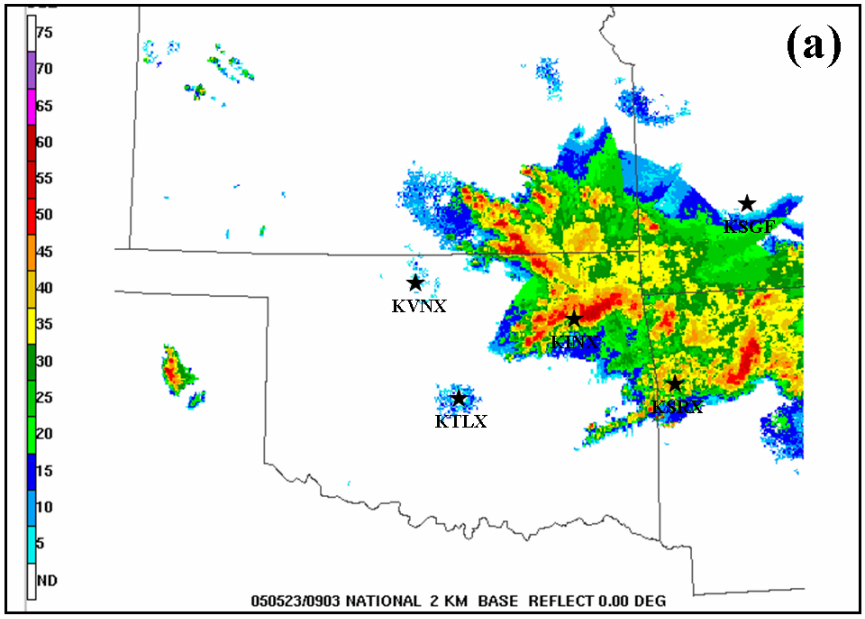

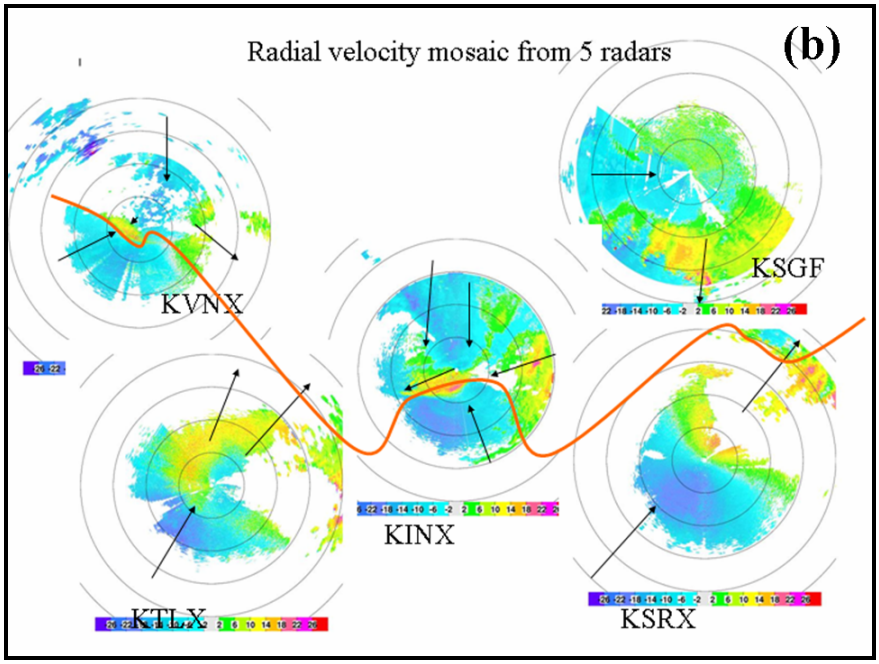

Fig. 1*. The mosaiced radar reflectivity field at 0900 UTC on 23 May 2005 (a) and a crude mosaic of radial velocity (b) from the five radars marked in (a).*

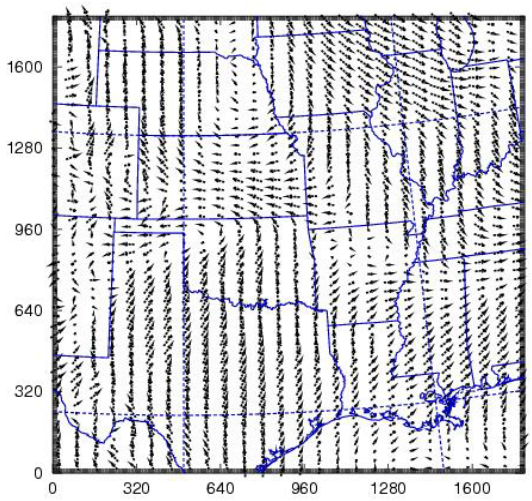

Fig. 2. *The experimental WRF-NMM analysis of near surface winds at 0900 UTC on 23 May 2005 that is used as the analysis background in this study.*

b. The grid-point statistial interpolation, GSI, system

The GSI analysis system is developed by Wu et al. (2002), which is a grid point version of the NCEP Spectral Statistical Interpolation (Parrish and Derber 1992) that is based on a 3D variational (3DVAR) algorithm. The cost function includes two terms and is defined by

$$J = 1/2[\mathbf{x}^T\mathbf{B}^{-1}\mathbf{x} + (H\mathbf{x}-\mathbf{y})\mathbf{R}^{-1}(H\mathbf{x}-\mathbf{y})], \qquad (8)$$

where the first term on the right hand side is the background constraint term and the second one is the observational term. The background term affects how the observational information spreads in space and overcomes underdetermined-ness problem associated with limited number of observations. Cross-correlations among the analysis variables can be and are often built into the analysis through the background error covariances in the background term too. The dimension of B matrix is however too large to calculate, store or manipulate explicitly, and is modeled using a recursive filter (Purser et al. 2003a; 2003b) in GSI. Variable transformation and preconditioning are also performed (Wu et al. 2002). The filter scales used by the recursive filter will impact analysis result, and will be examined in the next section.

3. A Real Case Study

a. Precipitation case of 23 May 2005

Radar radial velocity data collected by the five radars located in Oklahoma, Kansas and Missouri, on 23 May 2005 are used to examine the impact of radial velocity on GSI wind field analysis. On that day, two convective cells formed near 0300 UTC near the Kansas-Oklahoma boundary, along a frontal zone. It developed into a mesoscale convective system with precipitation near 0900 UTC. This precipitation system was observed by five WSR-88D radars: KTLX, KINX, KSRX, KSGF and KVNX. The radar locations and reflectivity mosaic at 0900 UTC is shown in Fig. 1a. The maximum of radar reflectivity reaches 60 dBZ. A crude mosaic of radial velocity from five radars is shown in Fig. 1b.

A wind shift-line in Fig. 1b is marked by a yellow curved line. Northerly winds dominate north of the wind shift line, while southwesterly winds dominate to the south. The precipitation region is mainly located mid-east of the analysis domain.

The 8 km resolution 0900 UTC WRF-NMM analyzed wind using GSI without radar data is shown in Fig. 2. There exists a wind shift line near the northern boundary of Oklahoma in the analysis. The location of this wind shift line is too far north compared to the location indicated by the radar observations. The dominant wind direction is southwesterly south of the wind shift line and is easterly on the north side. Convergence is weak along this line in the analysis.

To examine the impact of radar radial wind data on the GSI analysis, two sets of experiments are designed. The first set of experiments is to examine the impact of background error decorrelation length, while the second one is to examine the impact of the super-obs resolutions.

b. Impact of background error decorrelation length

In the first set of experiments, all observations from 5 radars are superobbed to a regular grid with a 0.1 degree resolution in the horizontal and a 500 m resolution in the vertical. We first examine the impact of the horizontal decorrelation length on the analysis. The default decorrelation length of the background errors used in GSI is estimated using the NMC method (Wu et al. 2002 and Wu 2005). The decorrelation length can be stretched by a stretching factor λ. In our experiments, λ is set to the default value of 1 in the control experiment and then to 0.25 in a sensitivity experiment. GSI analyses are obtained with above λ values, respectively, using the same background from the WRF-NMM analysis shown earlier for 0900 UTC and the super-obbed radial velocity data.

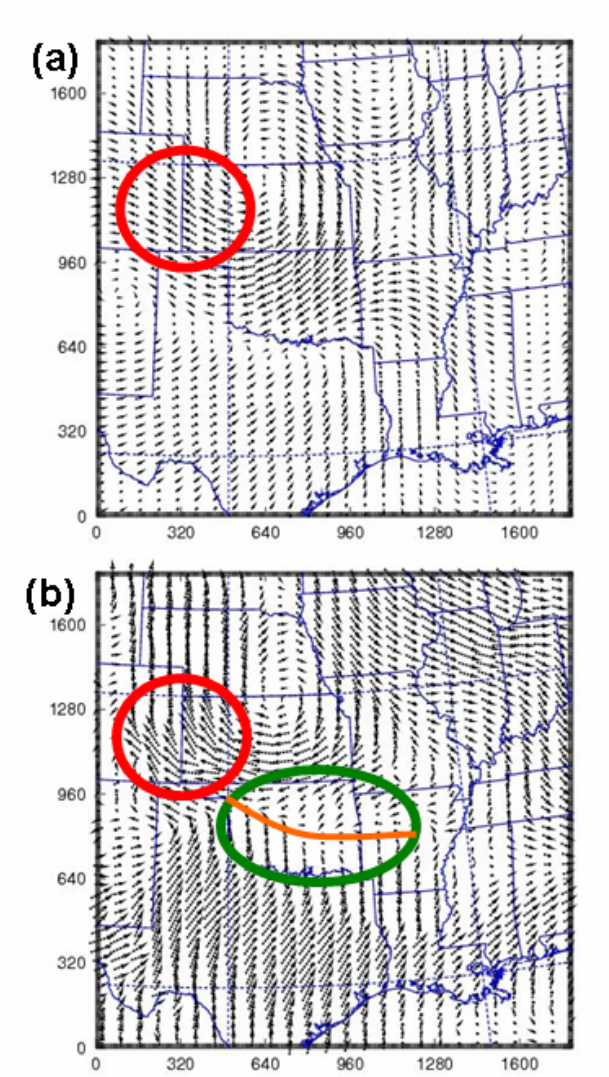

Fig. 3. *The GSI analyzed vector wind increment field (a) and full vector wind field (b) using default decorrelation length of background error.*

The GSI analysis increment and the analyzed vector wind field with $\lambda = 1$ are shown in Fig. 3. The analyzed increment (Fig. 3a) is very smooth and the observations are generally spread too far. Correspondingly, the analyzed wind vectors within closed red circle in Fig. 3b may not be correct and appear too large, which should be the result of inappropriate background error correlations as far as the radar data are concerned. The constraints in GSI also include one for modeling surface friction effect and it is parameterized as part of the background error and balance constraints. The balanced part of temperature, surface pressure and potential function are proportional to the increment of stream function, and the coupling parameters are estimated through regression using the differences between 48 and 24 hr forecasts verifying at the same time, i.e., the NMC method. These constraints are designed for large scale flows. For radar observations that represent convective scale flows, these relations may not be appropriate.

It is encouraging to see that the location of wind shift line in Fig. 3b is reasonable when radar data are included compared with that without using radar data in Fig. 2 and the dominant wind directions near the boundary of Oklahoma and Kansas becomes northeasterly. However, the convergence zone is too broad-over 200 km near the center of Oklahoma and very weak along the shift line.

It is clear that the analysis with $\lambda = 1$ is too smooth, a sensitivity experiment is therefore conducted with a reduced value of λ, at 0.25. which reduces the horizontal correlation length by a factor of 4. The GSI analyzed vector wind field and the analysis increment are shown in Fig. 4a and Fig. 4b, respectively. In comparison with the field in Fig. 3a, the wind shift line is now well-defined (Fig. 4a). In the analyzed wind field (Fig. 4b), much stronger and narrower convergence line is now found along the wind shift line and the strong winds inside red circles are reduced from those in the previous case.

These two experiments suggest that the default decorrelation length is too large for assimilating superobbed radar velocity. The radial velocity observational increments are spread too far and most of the convective-scale structures are filtered out. However, the assimilation is still very useful for capturing the convergence and wind shift line. After the analysis, the location of the wind shift line and the wind directions are both more realistic. When the decorrelation length is decreased to a more appropriate value, the convergence zone becomes narrower and the convergence becomes strong. The overall wind structure becomes much more realistic and corresponds better with the precipitation system along the line.

c. Impact of super-ob grid resolution

The resolution of superobs, in terms of the grid spacing used by the superobbing technique, is another factor that impacts the radial velocity assimilation. When the super-ob grid resolution decreases, super-obbed radial velocity represents the average of radial velocities within a larger domain, therefore, the represented fields is smoother and small-scale features is missing. When super-ob grid resolution increases, more detailed structure can be retained but the cost of analysis increases. Finding an optimal super-ob size that balances between cost and analysis quality is necessary.

The impact of the super-ob grid resolution on the analysis is examined in this subsection. In this set of experiments, the vertical resolution is fixed at 500 m and the horizontal resolution is set to 0.05, 0.1, 0.25

and 0.5 degree, correspondingly. Only results from two experiments that use super-ob horizontal resolutions of 0.05° and 0.5°, respectively, are presented here. Same as the above experiments, the super-obbed radial velocities are formed from the 5 radars. GSI analyses are then performed using λ=0.25 and the same background as used earlier.

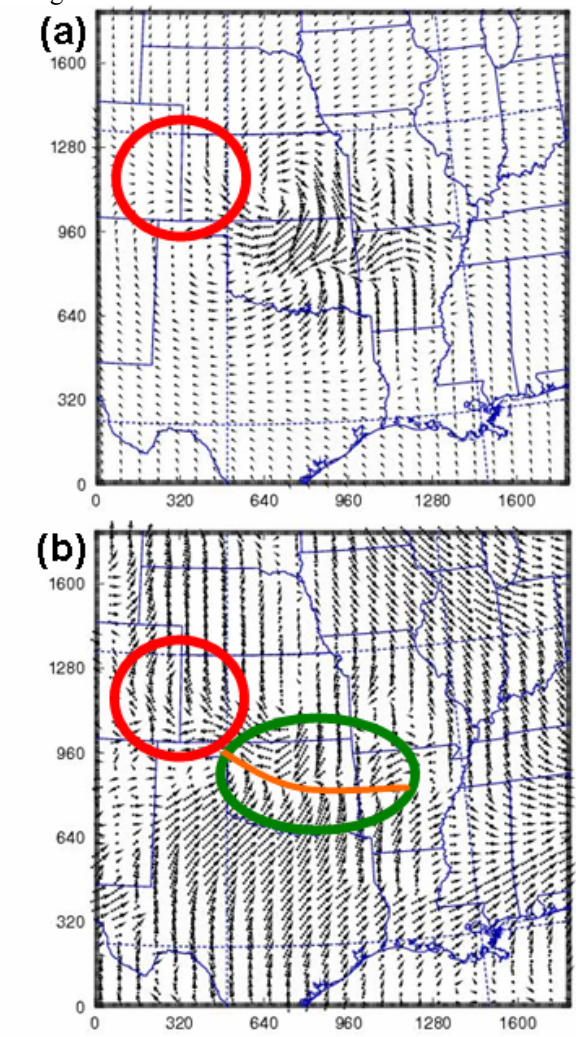

Fig. 4*. Same as Fig. 2 but with a decorrelation length of 0.25, a quarter of the default value.*

The GSI analysis with the 0.05° horizontal super-obbing resolution is shown in Fig. 5. As can be seen from Fig. 5a, the winds within the closed red circle are weaker than those in Fig. 4a. Because the super-ob grid resolution is high in this experiment, the number of super-obbed radial wind observations is 4 times that of observations analyzed in the previous experiments. When the number of the observations increases, the relative influence of the background constraint decreases, so are the influences of the built-in balance constraints. This explains why the winds in red circle are weaker, and closer to the radar observations. Comparing Fig. 5b with Fig. 1b the wind shift line in the GSI analysis matches the one indicated by the radar observations very well. In particular, the wind shift line curves bends towards the north at both ends, which agrees with the observations. This detailed structure is not clearly revealed, however, when the super-ob grid resolution is low.

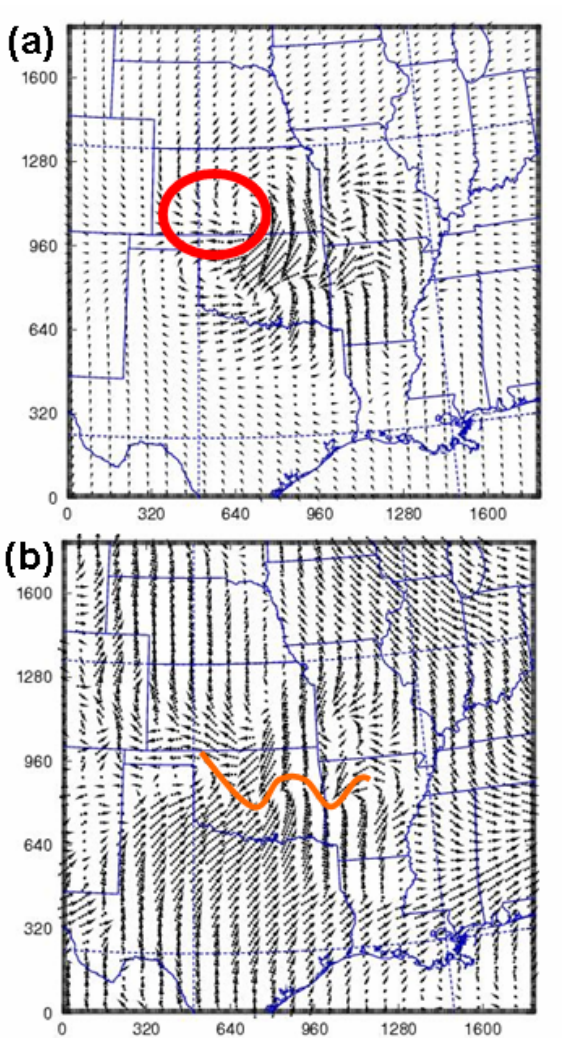

Fig. 5*. Same as Fig. 2 but for a super-ob resolution of 0.05° in the horizontal.*

The GSI analysis with a horizontal superob resolution of 0.5 ° is shown in Fig. 6. As can be seen from Fig. 6a, the analysis increment field is smoother than that in Fig. 3a, because the super-obbed radial velocity data now represent the means of larger regions. Some small-scale information is therefore missing in the analysis. The convergence of the analyzed field in Fig. 6a is clearly weaker than that seeing in Fig. 4a and 5a.

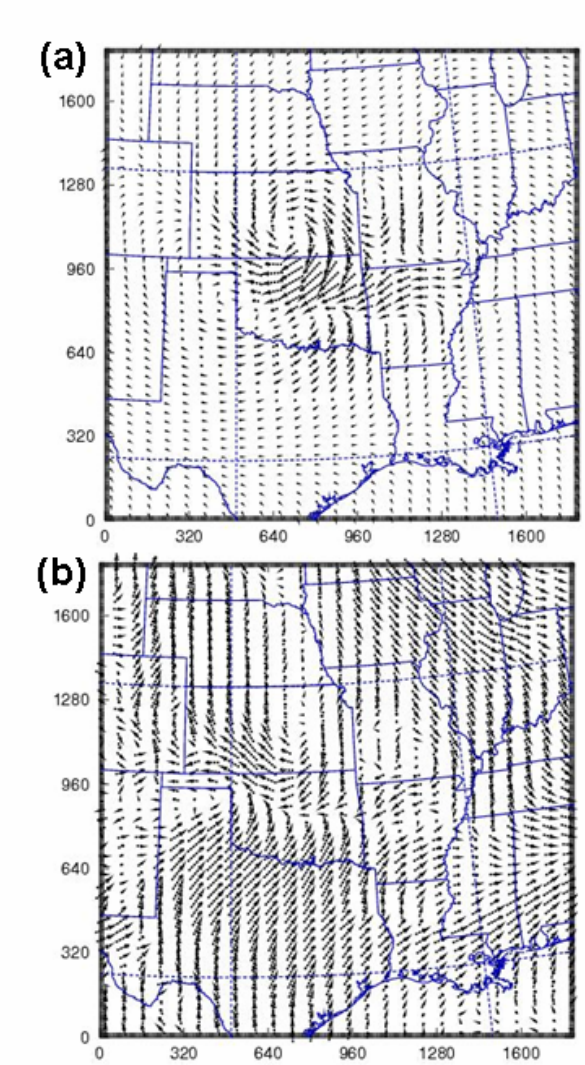

Fig. 6. *Same as Fig. 2 but for a super-ob resolution of 0.5° in the horizontal.*

5. Conclusions

In this paper, the NCEP GSI 3DVAR analysis is used to analyze super-obbed radial velocity data from 5 WSR-88D radars for a mesoscale convective system that occurred on 23 May 2005 in the Kansas-Oklahoma boundary. The background the experimental is real time analysis of GSI on an 8 km WRF-NMM grid. In a sense, this presents a multi-pass analysis procedure in which data used in the current experimental system are analyzed in the first pass while radar data are analyzed in the second pass.

The impacts of the error decorrelation length of the background and the radar data super-obbing size or resolution on the quality of analysis is examined. The results show the default decorrelation length is too large for the analysis of radar data, which typically contain many convective-scale structures. This causes an unreasonably smooth analysis, with grid points far away from the radar observations being incorrectly influenced by the data. The strong smoothing causes the loss of convective scale structures in the analysis and results in a too weak convergence line, even though the radar data still show beneficial effects in such a case. As the decorrelation length decreases, the convergence near the wind shift line becomes stronger and the overall wind analysis is significantly improved.

In addition, given the fixed and relatively small, decorrelation length, increasing super-ob grid resolution further improves the analysis. More detailed structures are obtained. On the contrary, decreasing the super-ob grid resolution results in the loss of the small-scale details contained in the radar observations.

The raw radar observations have high resolutions in both space and time, and often contain much small-scale information in the presence of precipitation. Such small-scale information obviously should not be spread too far in space and the default decorrelation length derived for large-scale analysis based on, e.g. the NMC method, is apparently not suitable for radar data assimilation. Estimation of suitable decorrelation length using high-resolution data sets and the application of anisotropic background error covariance are desirable and planned, and the impact of the radar data on short-term forecast will also be examined in the future.

Acknowledgments. This work was mainly supported by a DOT-FAA grant via DOC-NOAA NA17RJ1227. M. Xue and J. Gao were also supported by NSF grants ATM-0129892 and ATM-0331756. M. Xue was further supported by NSF ATM-0331594 and EEC-0313747.

References

Parrish, D. F. and J. C. Derber, 1992: The National Meteorological Center's spectral statistical-interpolation analysis system. *Mon. Wea. Rev.*, **120,** 1747-1763.

Parrish, D. F. 2005: Assimilation strategy for level 2 radar winds. *Presentation, 1st GSI User Orientation.* Camp spring, MD [available online at http://wwwt.emc.ncep.noaa.gov/gmb/treadon/gsi/documents/presentations/1st_gsi_orientation].

Purser, R. J., D. Parrish and M. Masutani, 2000: Meteorological observational data compression; an alternative to conventional "super-obbing". Office Note 430, National Centers for Environmental Prediction, Camp spring, MD [available online at http://wwwt.emc.ncep.noaa.gov/officenotes/FullTOC.html#2000]

Purser, R. J., W.-S. Wu, D. F. Parrish, and N. M. Roberts, 2003a: Numerical aspects of the

application of recursive filters to variational statistical analysis. Part I: Spatially homogeneous and isotropic Gaussian covariances. *Monthly Weather Review*, **131,** 1524-1535.

——, 2003b: Numerical aspects of the application of recursive filters to variational statistical

Wu, W.-S 2005: Background error and their estimation. *Presentation, 1st GSI User Orientation.* Camp spring, MD [available online at http://wwwt.emc.ncep.noaa.gov/gmb/treadon/gsi/documents/presentations/1st_gsi_orientation].

analysis. Part II: Spatially inhomogeneous and anisotropic general covariances. *Monthly Weather Review*, **131,** 1536-1548.

Wu, W.-S., R. J. Purser, and D. F. Parrish, 2002: Three-dimensional variational analysis with spatially inhomogeneous covariances. *Mon. Wea. Rev.*, **130,** 2905-2916.